

---

# Evaluation of six gas turbine evaporative cooling for Fars-Iran

A. A. Golneshan<sup>1</sup>, H. Nemati<sup>2\*</sup>

*1 Thermo-fluid Department, School of Mechanical Engineering,  
Shiraz University, Shiraz, Iran*

*2 Department of Mechanics, Marvdasht Branch, Islamic Azad University,  
Marvdasht, Iran*

*H.Nemati@miau.ac.ir*

---

*ABSTRACT. In this paper, effects of evaporative coolers on performances of six similar gas turbine power cycles were studied in one day. All required data were collected every five minutes from 09:00 till 16:00. Up to 12:00, evaporative coolers were out of services and therefore, there was a good chance to study the effect of evaporative coolers on a gas turbine under the operation. Moreover, since all these gas turbine power cycles are similar, the degree of uncertainty and validity of results are more judicable.*

*It was shown that besides the positive effect of cooling the inlet air, humidification by itself has an undeniable effect on increasing the power generation. Three parameters were assumed as the main sources of increasing the power generation in humidified condition: changes in the air mass flow rate, changes in the behavior of units equipment and finally changes in the air properties thermodynamically. Only the effect of the third parameter can be ignored.*

*RÉSUMÉ. Dans cet article, les effets des refroidisseurs à évaporation sur les performances de six cycles de puissance de turbine à gaz similaires ont été étudiés en une journée. Toutes les données requises ont été collectées toutes les cinq minutes de 09h00 à 16h00. Jusqu'à midi, les refroidisseurs à évaporation étaient hors service et il était donc tout à fait possible d'étudier l'effet des refroidisseurs à évaporation sur une turbine à gaz en cours d'exploitation. De plus, comme tous ces cycles de puissance des turbines à gaz sont similaires, le degré d'incertitude et la validité des résultats sont plus probants. Il a été démontré que, outre l'effet positif du refroidissement de l'air d'entrée, l'humidification a en soi un effet indéniable sur l'augmentation de la production d'énergie. Trois paramètres ont été supposés être les principales sources d'augmentation de la production d'électricité en condition humidifiée: les changements du débit massique de l'air, les changements du comportement des équipements des unités et enfin les changements thermodynamiques des propriétés de l'air. Seul l'effet du troisième paramètre peut être ignoré.*

*KEYWORDS: evaporative cooler, gas turbine, humidification, ideality coefficient.*

*MOTS-CLÉS: refroidisseur à évaporation, turbine à gaz, humidification, coefficient d'idéal.*

---

DOI:10.3166/ACSM.42.281-301 © 2018 Lavoisier

## 1. Introduction

The gas turbine is one of the most comprehensive tools in the power generation industry. Its compactness beside high power-to-weight ratio and ease of installation makes it incomparable. So, researchers are working hard to improve the efficiency a GTG (gas turbine generator). Review of some improvements in gas turbine materials and technologies may be found in Ref.(Poullikkas, 2005). Commonly, the efficiency of a gas turbine is varying between 32 to 42 % (Mohapatra, 2013).

Several methods may be found to improve the efficiency (Gulotta *et al.*, 2017; Gulotta *et al.*, 2018). Out of the various methods of cycle improvement, it is proven that air inlet temperate reduction results in a reduction of required compressor work. The compressor consumes approximately two-thirds of the GTG power production (Carmona, 2015). So, reduction in required compressor work increases the net power output significantly. On the other hand, since the air temperature reduction increases the air density, it causes the intake mass flow rate increases also. So the total generated power is increased also.

One option to increase the mass flow rate and decrease the air intake temperature is injecting fine water droplets into the inlet air stream. Water droplets decrease the air temperature through an adiabatic heat and mass exchange process.

De Lucia *et al.* (1995) have studied gas turbines with inlet air cooling. They concluded that evaporative cooling increases power production by about 4 % per year. Najjar (1996) claimed that by means of absorption inlet cooling the power output increases by about 21%. Bassily (2001) performed energy balance analysis and concluded that indirect or evaporative inlet-air increases the performance significantly. Wang and Chiou (2004) calculated the inlet cooling from 305 to 283K increases power output by about 12 % and efficiency about 5.16%. Thermodynamics of fogging systems are analyzed in Ref. (Chaker *et al.*, 2002) and (Cataldi *et al.*, 2006).

A general misconception is that evaporative cooling works only in warm climates to reduce air inlet temperature. So, it is not utilized in the early morning in which the air temperature is relatively lower. In this research, the effect of evaporative coolers has been studied deeply based on real data collected from similar six gas turbine cycle under operation.

## 2. Plant description

Fars power plant is comprised of six gas units and the capacity of each unit is 123.4 MW. A schematic diagram of a gas turbine cycle with inlet air evaporative cooler is shown in Fig. 1. Filtered ambient air is humidified and cooled by an evaporative cooler. This evaporative cooler comes into the service only when the ambient temperature exceeds 40°C. The fogging system in evaporative cooler sprays tiny droplets into the air and decreases the inlet air stream to the compressor and meanwhile increases its humidity. Humidified air pressure increases in the compressor, and is conducted to the combustion chamber.

In the combustion chamber, the temperature increases in an approximately isobaric process. The main source of fuel used in the combustion chamber is natural gas. The flue gas exits the combustion chamber to the turbine. Exhausted gas generates work in the turbine. Since the air moisture content can not be ignored, the combustion in the combustion chamber must be simulated thermodynamically and using fuel low heating value in conjugated with the of dry air assumption which is a common method is not applicable here.

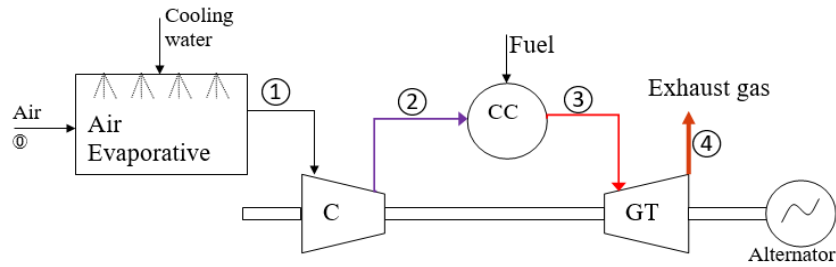


Figure 1. Schematic diagram of a gas turbine cycle with an evaporative cooler

### 2.1. Evaporative cooler model

Specific enthalpy of the wet air stream per unit mass of dry air before and after the evaporative cooler is:

$$h_0 = h_{air0} + \frac{h_{water0}}{18\omega_0} \quad (1)$$

$$h_1 = h_{air1} + \frac{h_{water1}}{18\omega_1} \quad (2)$$

In which  $\omega$  is the specific humidity of air stream at the indicated point. With the assumption of the adiabatic evaporative cooler, applying the energy balance equation across the evaporative cooler control volume boundary gives:

$$\omega_1 = \frac{\omega_0 [h_{water}(P_w, T_0) - h_{f,water}(T_0)] - cp_{air0,1} [T_1 - T_0]}{[h_{g,water}(T_1) - h_{f,water}(T_0)]} \quad (3)$$

$h_{g,water}$  and  $h_{f,water}$  are the water vapor and liquid specific enthalpy at the saturated condition and  $cp_{air0,1}$  is the dry air constant specific heat at the average temperature between  $T_0$  and  $T_1$ . In Eq. 3, the water partial pressure,  $P_w$ , is calculated by (Borgnakke and Sonntag, 2016):

$$P_w = \phi_0 P_{sat,water,0} \quad (4)$$

$$\phi_0 = \frac{\omega_0 P_0}{(0.622 + \omega_0) P_{sat,water,0}} \quad (5)$$

$P_{sat,water,0}$  is the water saturated pressure at Temperature  $T_0$ . It is clear that whenever the evaporative coolers are off,  $w=w_0$ , and otherwise  $w=w_1$ .

The inlet vapor flow rate to the gas unit is:

$$\dot{m}_{v,0} = \dot{m}_{dry\_air} \omega_0 \quad (6)$$

and in the same way, the vapor flow rate into the compressor is:

$$\dot{m}_{v,1} = \dot{m}_{dry\_air} \omega_1 \quad (7)$$

Finally, the total air flow rate into the compressor is:

$$\dot{m}_{air} = \dot{m}_{dry\_air} + \dot{m}_{v,1} \quad (8)$$

## 2.2. Wet air model

Air and water vapor in the air are assumed as an ideal gas. So, it can be assumed that their properties vary only with temperature. Introducing  $\theta = T/100$  ( $T$  in Kelvin), the air constant pressure specific heat is (Ibrahim *et al.*, 2017):

$$c_{p,air} = (1.04841 - 3.8371 \frac{\theta}{10^3} + 9.4537 \frac{\theta^2}{10^5} - 5.4931 \frac{\theta^3}{10^7} + 7.9218 \frac{\theta^4}{10^{10}}) \quad (9)$$

and for water vapor:

$$c_{p,H_2O} = [143.05 - 183.54\theta^{0.25} + 82.751\theta^{0.5} - 3.6989\theta] / 18.015 \quad (10)$$

The water vapor specific enthalpy (kJ/kmol) is:

$$h_{H_2O} = \begin{cases} -9903.9842 + 3250.3251\theta + 42.806253\theta^2 - 6.2183832\theta^3 & \theta < 3 \\ -9598 + 3094\theta + 42\theta^2 & 3 \leq \theta \leq 4 \\ -9494.7937 + 3083.6892\theta + 31.208332\theta^2 + 1.9537038\theta^3 & 4 < \theta < 10 \\ -0.04166667\theta^4 & \\ -10205.43 + 2943.4614\theta + 73.011089\theta^2 - 0.63909098\theta^3 & \theta \geq 10 \end{cases} \quad (11)$$

## 2.3. Compressor model

In an ideal compressor with no entropy generation or exergy destruction, the compressor isentropic pressure ratio can be calculated as:

$$\left(\frac{P_{2s}}{P_1}\right) = \left[\frac{T_2}{T_1}\right]^{cp_{2mix}/R_{mix}} \quad (12)$$

in which  $P_{2s}$  is compressor isentropic outlet pressure.

$$cp_{2mix} = \frac{cp_{air1,2} + cp_{H_2O1,2}\omega_1}{1 + \omega_1} \quad (13)$$

$cp_{air1,2}$  and  $cp_{H_2O1,2}$  are the air and water vapor constant pressure specific heat at the average temperature between  $T_1$  and  $T_2$ .

$$R_{mix} = \frac{R_{air} + R_{water}\omega_1}{1 + \omega_1} \quad (14)$$

To compare compressors with each other,  $\kappa_c$  may be introduced.  $\kappa_c$  is defined as the ratio of isentropic to real compressor outlet pressure. Consequently, it shows how far the compressor outlet pressure is from isentropic outlet pressure:

$$\kappa_c = \frac{P_{2s}}{P_2} \quad (15)$$

#### 2.4. Combustion chamber model

Based on the fuel analysis, the natural gas components used as fuel are:

Table 1. Fuel content

	C1	C2	C3	N2
Mole Fraction%	89.19	4.1	1.21	5.5
Formation Enthalpy (kJ/kmol) (Borgnakke and Sonntag, 2016)	-74873	-84740	-103900	0
Molecular Weight (kmol/kg) (Borgnakke and Sonntag, 2016)	16.043	30.07	44.097	28.0135

With the assumption of complete combustion (this assumption was validated by analysis of exit gas from the stack), the flue gas contents are:

The combustion in the combustion chamber can be simulated thermodynamically as:

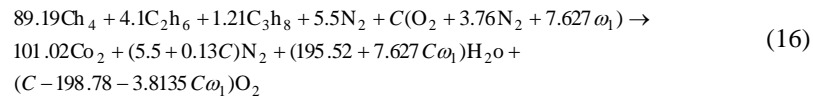


Table 2. The flue gas contents

	CO <sub>2</sub>	H <sub>2</sub> O	N <sub>2</sub>
Mole	1.0102	1.9552	7.52913
Formation Enthalpy (kJ/kmol) [18]	393522	241826	0
Molecular Weight (kmol/kg) [18]	44.01	18	28.0135
<i>R</i> (kJ/kgK) [18]	0.1889	0.4615	0.2968

Performed energy balance analysis over combustion chamber control volume:

$$\sum_i \dot{n}_i [h_f + \{h(T_3) - h(298.15\text{K})\}]_i - \sum_j \dot{n}_j [h_f + \{h(T_3) - h(298.15\text{K})\}]_j = \dot{Q} \quad (17)$$

In the above equation  $h_f$  is the formation enthalpy and  $i$  and  $j$ , indicates to the  $i^{\text{th}}$  component of reactants and the  $j^{\text{th}}$  component of products in the combustion chamber respectively.  $Q$  is the released heat for each mole of fuel.

Introducing  $x_i$  as mass fraction,  $J_i$  as mole fraction and  $W_i$  as molar mass of  $i^{\text{th}}$  component as well as  $W_{fuel}$  as fuel molar mass, the thermodynamic properties of flue gas will be:

$$cp_{1,flu} = \frac{\left\{ \begin{array}{l} (x_{Co_2} cp_{Co_2} + x_{H_2O} cp_{H_2O} + (x_{N_2} + 3.76 CW_{N_2}) cp_{N_2} + \\ 7.63 C \omega_1 W_{H_2O} cp_{H_2O} + (C - J_{O_2}) W_{O_2} cp_{O_2} \end{array} \right\}}{(1 + \omega_1)(137.33C) + W_{fuel}} \quad (18)$$

All used properties are evaluated at the turbine outlet temperature.  $C$  is the mole of air (including excess air) to burn each mole of fuel.  $R$ -value of flue gas is also calculated as follows:

$$R_{flu} = \frac{\left\{ \begin{array}{l} R_{Co_2} x_{Co_2} + R_{H_2O} x_{H_2O} + (x_{N_2} + 3.76 CW_{N_2}) R_{N_2} + \\ 7.63 C \omega_1 W_{H_2O} R_{H_2O} + (C - J_{O_2}) W_{O_2} R_{O_2} \end{array} \right\}}{(1 + \omega_1)(137.33 C) + 100 W_{Fuel}} \quad (19)$$

In the same way,  $cp_{2,flu}$  can also be evaluated at the combustion chamber outlet temperature.

### 2.5. Flue gas component model

The thermodynamic properties used in the previous part depends on temperature. Introducing  $\theta = T/100$  ( $T$  in Kelvin), the constant pressure specific heats are (Borgnakke and Sonntag, 2016):

$$cp_{N_2} = \left[ 39.06 - 512.79\theta^{-1.5} + 1072.7\theta^{-2} - 820.4\theta^{-3} \right] / 28.013 \text{ (kJ/kgK)} \quad (20)$$

$$cp_{O_2} = \left[ 37.432 + 0.020102\theta^{1.5} - 178.57\theta^{-1.5} + 236.88\theta^{-2} \right] / 31.999 \text{ (kJ/kgK)} \quad (21)$$

$$cp_{CO_2} = \left[ -3.7357 + 30.529\theta^{0.5} - 4.1034\theta + 0.024198\theta^2 \right] / 44.01 \text{ (kJ/kgK)} \quad (22)$$

$$cp_{CH_4} = \left[ -672.87 + 439.74\theta^{0.25} - 24.875\theta^{0.75} + 323.88\theta^{0.5} \right] / 16.04 \text{ (kJ/kgK)} \quad (23)$$

$$cp_{C_2H_6} = \left[ 6.895 + 17.26\theta - 0.6402\theta^2 + 0.00728\theta^3 \right] / 30.07 \text{ (kJ/kgK)} \quad (24)$$

$$cp_{C_3H_8} = \left[ -4.042 + 30.46\theta - 1.571\theta^2 + 0.03171\theta^3 \right] / 44.09 \text{ (kJ/kgK)} \quad (25)$$

$$cp_{C_4H_{10}} = \left[ 3.954 + 37.12\theta - 1.833\theta^2 + 0.03498\theta^3 \right] / 58.124 \text{ (kJ/kgK)} \quad (26)$$

and based on curve fitting according to thermodynamic table (Borgnakke and Sonntag, 2016),

$$h_{air} = 4.666416 + 0.9683\theta + 3.961 \times 10^{-5}\theta^2 + 3.2648 \times 10^{-8}\theta^3 \text{ (kJ/kgK)} \quad (27)$$

$$h_{N_2} \text{ (kJ/kgK)} = \begin{cases} -40848385.458 + 136669780^{1.0024978} / (4711.4676 + \theta^{1.0024978}) & \theta \leq 4 \\ -8670 + 2923.5942\theta - 12.044984\theta^2 + 2.136434\theta^3 & 4 < \theta < 10 \\ \exp\left(8.0789435 - \frac{4.8921249}{\theta} + 1.0352864 \ln(\theta)\right) & \theta \geq 10 \end{cases} \quad (28)$$

$$h_{O_2} \text{ (kJ/kgK)} = \begin{cases} -8683.2986 + 2915.5857\theta - 11.791232\theta^2 + 3.6922661\theta^3 & 3 < \theta \\ -8349 + 2672\theta + 43\theta^2 & 3 \leq \theta \leq 4 \\ -7939.7229 + 2451.347\theta + 80.132035\theta^2 - 1.8838384\theta^3 & 4 < \theta < 10 \\ -8879.333 + 2882.7507\theta + 31.329828\theta^2 - 0.28252785\theta^3 & \theta \geq 10 \end{cases} \quad (29)$$

$$h_{CO_2} \text{ (kJ/kgK)} = \begin{cases} -9363.977 + 2939.3076\theta - 83.011986\theta^2 + 50.577468\theta^3 & \theta < 3 \\ -9525 + 2646\theta + 184\theta^2 & 3 \leq \theta \leq 4 \\ -9584.9286 + 2538.8571\theta + 240.08333\theta^2 - 6.41667\theta^3 & 4 < \theta < 10 \\ \exp\left(8.6546661 - \frac{5.9395707}{\theta} + 1.0233514 \ln(\theta)\right) & \theta \geq 10 \end{cases} \quad (30)$$

## 2.6. Turbine model

Flue gas specific enthalpy to the turbine can be calculated by the following equation:

$$h_4 = \frac{J_{Co_2}h_{Co_2} + J_{H_2O}h_{H_2O} + (C - J_{O_2})h_{O_2} + (J_{N_2} + 3.76C)h_{N_2} + 7.627C\omega_1h_{H_2O}}{137.33C} \quad (31)$$

in which all the thermodynamic properties are evaluated at temperature  $T_1$ . In the same way,  $h_3$  may be calculated at the combustion chamber temperature,  $T_3$ .

It is assumed that  $p_2 \approx p_3$  and  $p_1 \approx p_4$ . Based on isentropic turbine equation and similar to Eq. 15,  $\kappa_t$  is introduced as below:

$$\kappa_t = \left[ \frac{T_3}{T_4} \right]^{cp_{3,flu}/R_{flu}} \left( \frac{P_2}{P_1} \right) \quad (32)$$

Knowing the fuel component as well as fuel mass flow rate,  $m_{Fuel}$ , dry air mass flow rate will be:

$$\dot{m}_{dry\_air} = \frac{\dot{m}_{Fuel}}{W_{Fuel}C \times 28.851 \times 4.76} \quad (33)$$

and therefore, the electricity generated power is:

$$\dot{W}_E = \dot{m}_{dry\_air} [(h_3 - h_4) - (h_2 - h_1)] \eta_{Gen} \quad (34)$$

in which  $\eta_{Gen}$  is the generator efficiency.

### 3. Methodology

In the above equations, both  $T_3$ ,  $C$  are unknown parameters. So, at first, an initial value for  $T_3$  is assumed.  $C$  and after that,  $\dot{m}_{dry\_air}$  are evaluated based on this assumption and eventually,  $W_E$  is calculated using Eq. 34. This procedure repeats till the calculated value of  $W_E$  gets equal to its measured value.

For the six similar gas turbines, the temperature and pressure of all components were measured on 27th July. Measuring process started from 09:00 till 16:00 for every five minutes. A sample of measuring data has been shown in Appendix A.

### 4. Results and discussion

Using the above equations, the performance of each component is studied deeply. The evaporative cooler is the first equipment which has been studied. Fortunately, evaporative cooler comes into the service only at noon. So, it provides a valuable chance to compare the effect of water injection on the air stream in one day. Finally, the overall plant efficiency in the presence and absence of evaporative cooler has been studied.

In Fig. 2, compressors entrance temperatures temperature, as well as ambient temperature, have been presented. According to this figure, the ambient temperature

changes 10°C from about 30°C at 9:00 to about 40°C at noon. Before starting evaporative cooler, the ambient temperature and the inlet air temperature are approximately the same. At 12:00, when evaporative coolers come into service, the inlet temperature drops suddenly more than 10°C and after that, it remains constant approximately.

However, their cooling effects are not the same. Evaporative cooler of the 1st unit decreases the temperature from 40°C to 22°C, while in cooler number 3 or number 6, the air temperate reduces from 38°C to 30°C. These variations in evaporative coolers performances provide a valuable chance to study the effect of moisture content on the GTG performance.

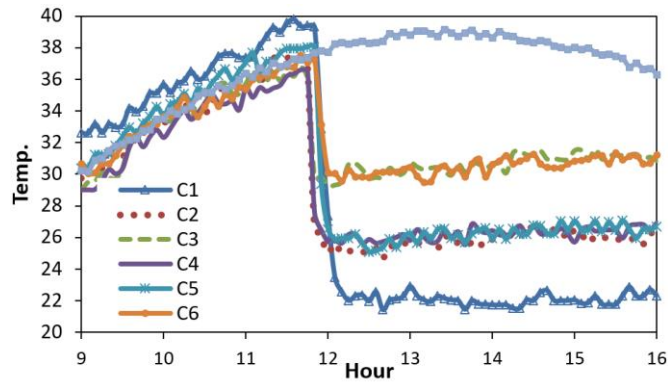


Figure 2. Variations of ambient and compressors inlet temperature in one day

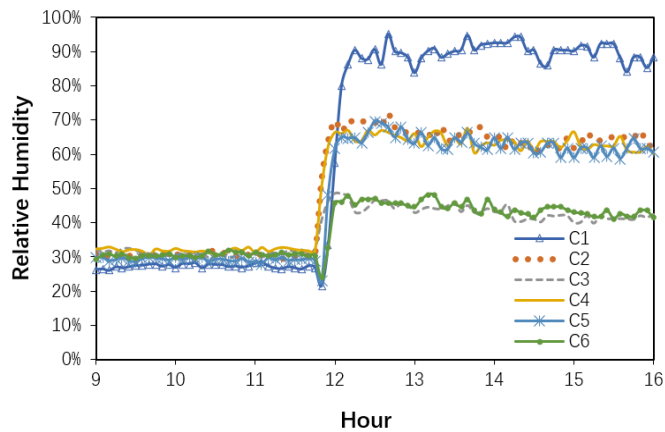


Figure 3. Variations of compressors inlet relative humidity in one day

Since in an evaporative cooler, the reduction of temperature is mainly due to an increase in the air humidity ratio, it is expected to have different air relative humidity in the inlet of each compressor. Fig. 3 shows relative humidity for each compressor inlet air. The relative humidity of cooler number 1 reaches to about 93%. This value for coolers number 2, 4 and 5 is something between 60% and 70%. For cooler 3 and 6 this value is about 45%. This means that ambient air humidity only increased by 15%.

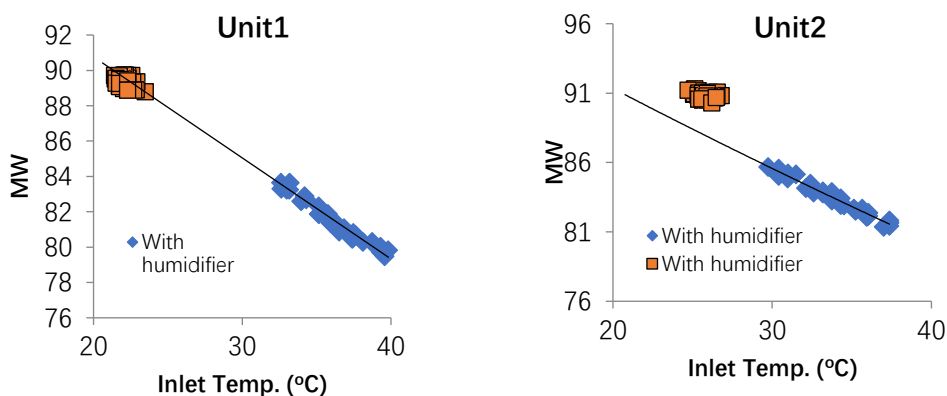
The generated power in each unit for both conditions (with and without evaporative cooler) is shown in Fig. 4. According to this Fig. 4, by increasing the ambient temperature, the generated power decreases significantly. While the temperature increases from around 30 °C to nearly 38°C, the generated power in different units decreases something between 5 to 9%. When the evaporative cooler comes into the service in each unit, inlet temperature reduces considerably and the generated power jumps suddenly.

Solid lines in Figure. 4 show the approximate trends of generated powers vs. temperatures. In all units except unit 1, jumps in the generated powers are more than expected values. In unit 1, the generated value is aligned approximately with the predicted value. Among all units, the behavior of unit 3 is worthwhile to note. Due to the poor performance of its evaporative cooler, the humidified air temperature is approximately the same as air temperature in the morning. However, the generated power in the wet condition is considerably more than the morning.

Three sources can be assumed that have main roles in increasing the power generation in humidified condition:

- Changes in the air mass flow rate.
- Changes in the behavior of units equipment encountering humidified stream.
- Changes in the air properties thermodynamically.

In the following, each one has been studied deeply.



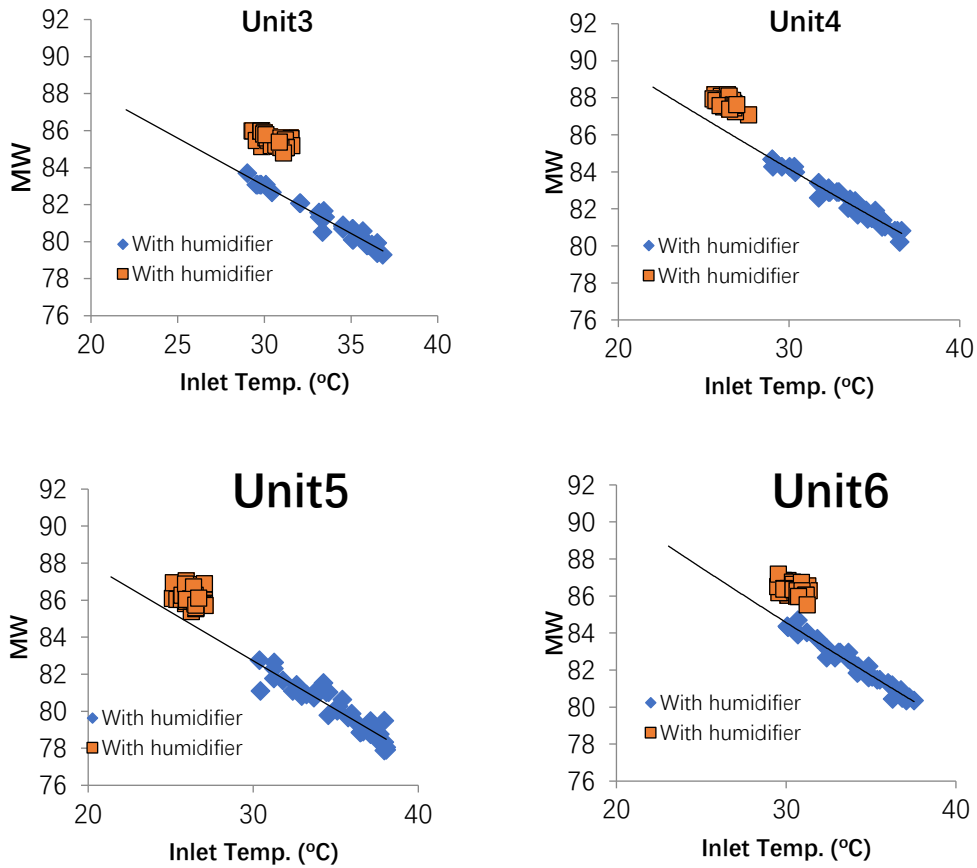


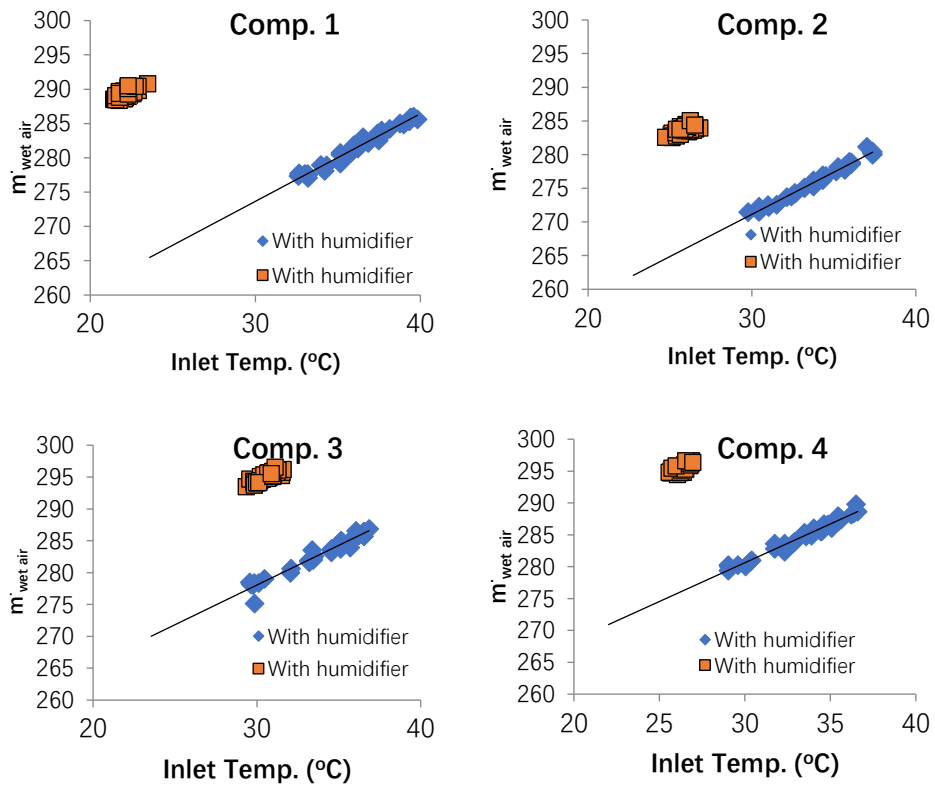
Figure 4. Generated power vs. inlet air temperature in one day

#### 4.1. Changes in the air mass flow rate

The air temperature affects the air density whereupon mass flow rate changes. However, humidifying the air increases the air mass flow rate by two distinct methods: by increasing the air density due to reducing its temperature and also by increasing the moisture content. Fig. 5 shows the inlet air mass flow rate to each compressor. Based on the logic of power plant control systems, the air mass flow rate reduces about 3 to 4 % due to ambient temperature increase. In this figure, solid lines show the approximate trends of these variations. As it is clear, the humidifying increases the air flow rate among 5% to 20% more than the predicted value. Again, mass flow rates in both Compressor 3 and 6 are subject to interest. While temperatures are the same in without and with evaporative coolers, the mass flow rates of humidified air

are much more than times in which evaporative coolers are off. All in all, it can be concluded that increasing the mass flow rate has a significant effect on power generation improvement. However, it is still required to make it clear if the increase in the mass flow rate is the main source of generation improvement or not?

To answer this question, the generated power for each kg of the air stream is plotted against air inlet temperature for each unit in Fig. 6. With the exception of unit 3 and unit 6 for them, the evaporative cooler performances are not as great as others; the generated power per each kg of air while the evaporative cooler is in the service is less. So, it can be concluded that the generated power does not increase as much as the flow rate increases. The readers shall not hesitate to the positive effect of the evaporative cooler by this conclusion. To clear this, the average mass flow rate of consumed fuel to the average mass flow rate of air for each unit has been shown in Fig. 7. The most increase in this ratio can be observed in unit 1 which is less than 3.5%. For other units, the increase in this ratio is less than 2.5%. So, the increase in fuel consumption is less than the increase in air mass flow rate. Based on this discussion, it can be concluded that changes in the behavior of units equipment encountering humidified stream are undeniable. This fact is discussed in the next part.



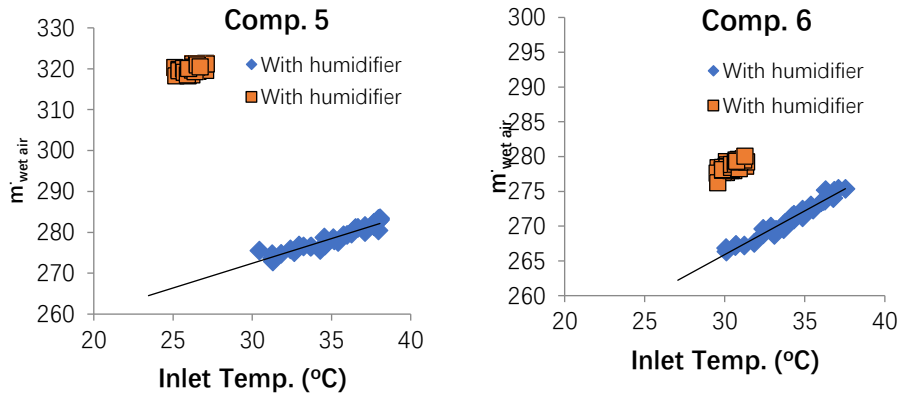
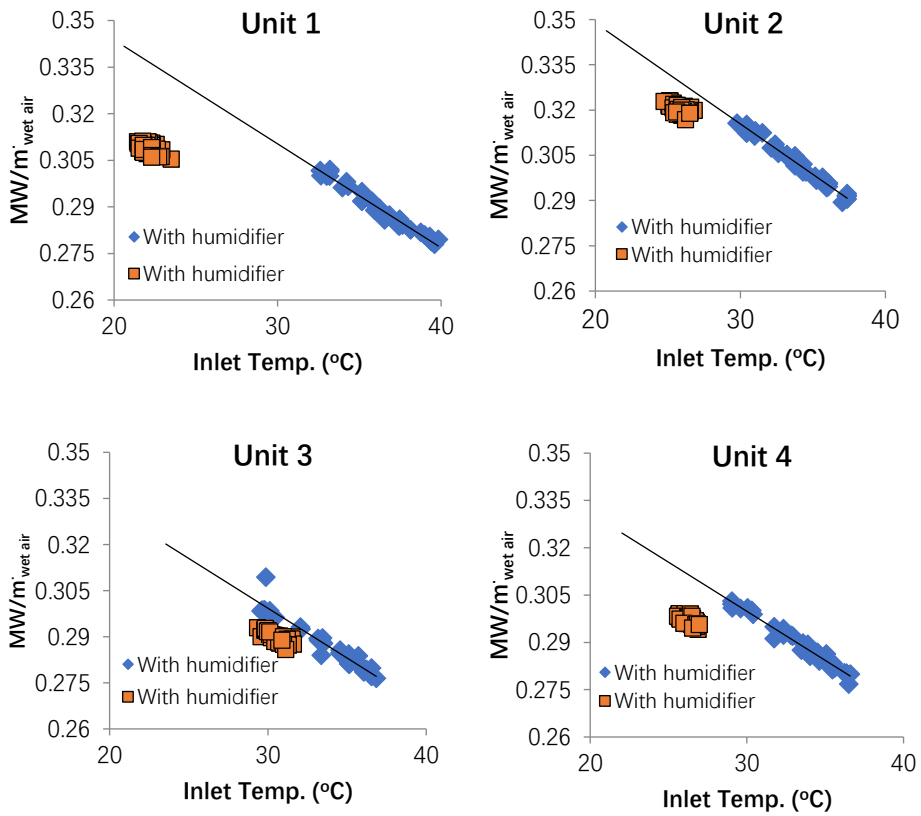


Figure 5. Air mass flow rate vs. inlet air temperature in one day



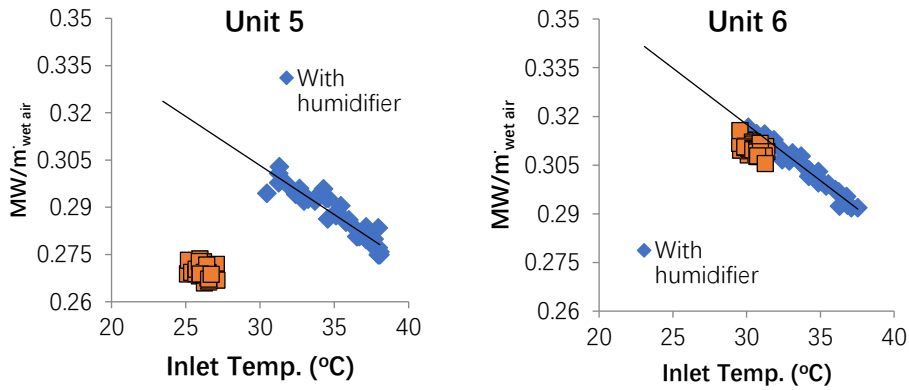


Figure 6. Generated power per kg of air vs. inlet air temperature in one day

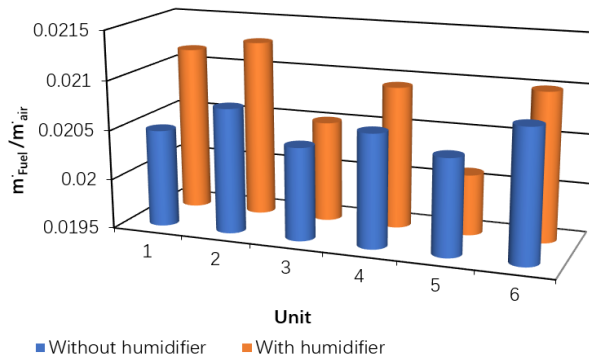


Figure 7. Fuel to air mass ratio for each unit

#### 4.2. Changes in the behavior of units equipment

Besides the air mass flow rate value, another parameter that affects the power generation is the compression ratio. For each unit, the compression ratio of the compressor is shown in Fig. 8. Solid lines show the approximate trends of variations of compression ratios against inlet temperature. Except for unit 1, the compression ratio of humidified air is considerably more than the predicted value. This shows that these compressors operate better in humidified air. For compressor 1, the predicted value and the measured one is approximately the same.

Again, the behaviors of units 3 and 6 are interesting. Although the humidified air

temperature and the air temperature in that morning are approximately the same, the compression ratio in the presence of evaporative cooler is more. To investigate the ideality of each compressor,  $\kappa_c$ , as described in Eq. (15) is a useful tool. Rewriting Eq. (15) and Eq. (12) yields:

$$P_2 = \frac{P_1}{\kappa_c} \left[ \frac{T_2}{T_1} \right]^{cp_{2mix}/R_{mix}} \quad (35)$$

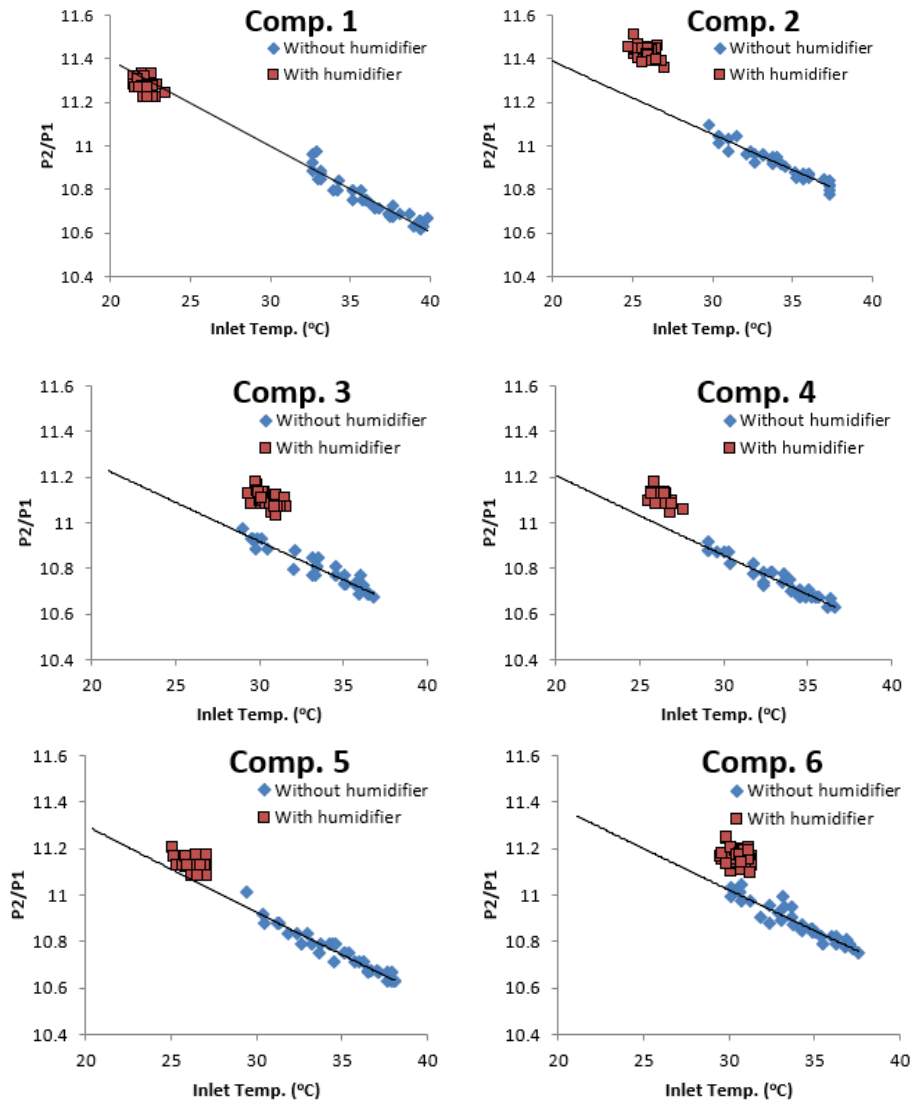


Figure 8. Compression ratio vs. inlet air temperature in one day

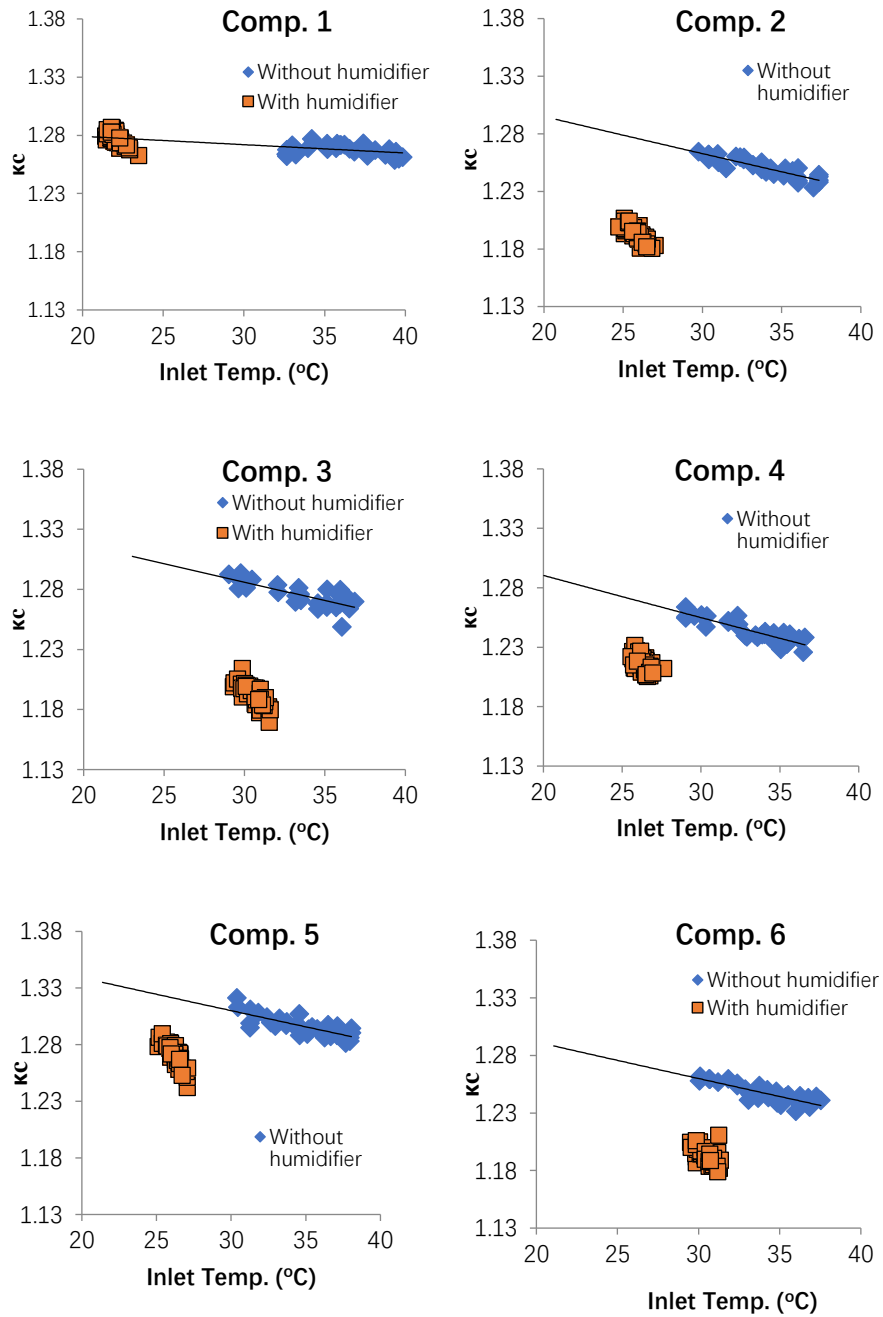


Figure 9. Compressor ideality coefficient vs. inlet air temperature in one day

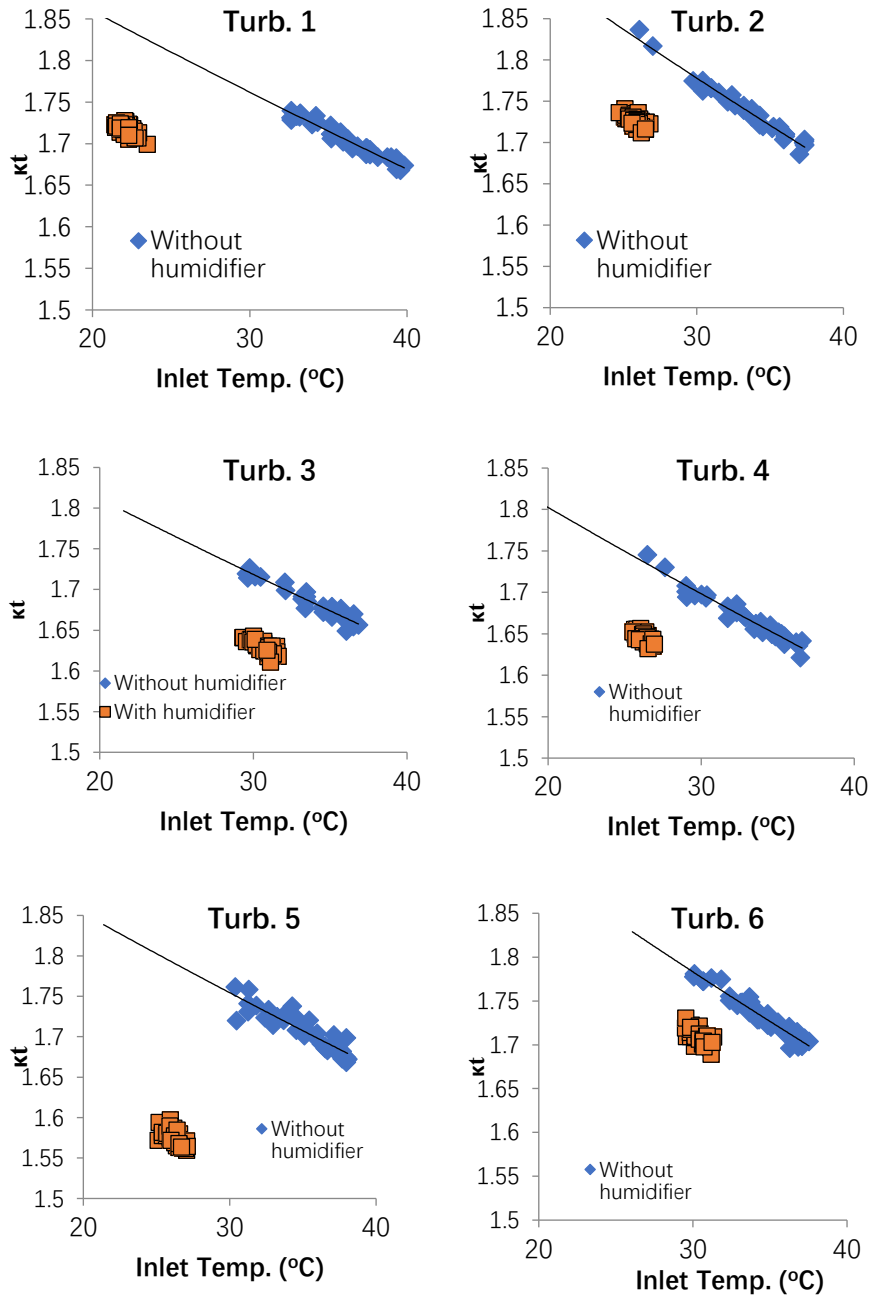


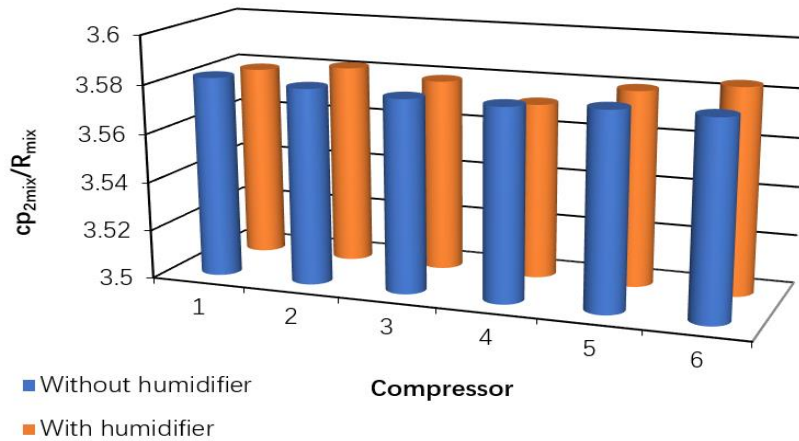
Figure 10. Turbine ideality coefficient vs. inlet air temperature in one day

Based on Eq. (35) the compressor exit pressure may be separated into two ideal and non-ideal parts.  $P_1 [T_2/T_1]^{\frac{cp_{2mix}}{R_{mix}}}$  is the isentropic part of pressure (ideal part) and all non-idealities are collected in the coefficient  $\kappa_c$ . So, whatever it is close to unity, the compressor is closer to the isentropic condition.

Fig. 9 Shows  $\kappa_c$  against inlet temperature. Except compressor 1,  $\kappa_c$  in all others are closer to unity not only in comparison to predicted values but also in comparison to that morning working condition. The reason for this behavior is not clear. Maybe the size of droplet or traditional mark of compressor affects superiority of  $\kappa_c$  in the presence of evaporative cooler. However, it can be asserted that at least, for the current power plant, the presence of evaporative cooler improves compressor performance. Figure 10 also shows  $\kappa_t$  against inlet temperature for each turbine. More or less, the same results can be concluded.

**4.3. Changes in the air properties thermodynamically**

The last object which is studied here is changes in thermodynamic properties due to moisture content. Based on Eq. (12) and Eq. (32) the main thermodynamic parameter which may affect the power generation is  $\frac{cp_{2mix}}{R_{mix}}$  for the compressor and  $\frac{cp_{3flu}}{R_{flu}}$  for the turbine. These values have been shown in Figure 11. Based on this figure, these parameters have not been changed considerably. So, it can not be expected that these parameters affect the compression ratio.



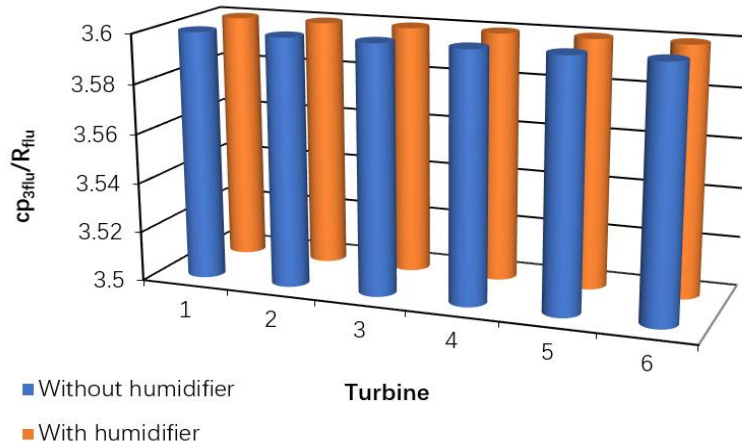


Figure 11. Compressor and turbine thermodynamic effecting parameters

## 5. Conclusion

In this study, effects of air evaporative coolers were studied deeply for six similar gas turbines. In one day, required data were measured and collected every five minutes. Since the evaporative coolers are absent in the morning, it provides a good chance to compare their effects on the power generation. Moreover, since these gas turbines are exactly the same, it is promising to have validated results.

It was found out the power generation is increased among 2% to 3% relative to expected value at that cool temperature.

It was shown that the increase in the mass flow rate is one of the main parameters in increasing the power generation. Based on the collected data, the humidifying increases the air flow rate among 5% to 20% more than the predicted value.

The other factor which is worthwhile to mention is the change in compressor and turbine behavior in the presence of an evaporative cooler. It was shown that the compression ratio in the cycle with humidified air is considerably more than the expected value.

All in all, it can be concluded that using evaporative cooler increases the gas turbine power plant performance. The last point is that it can be claimed that the effect of an evaporative cooler in increasing power generation is not summarized only in its cooling effect. It was shown that besides its cooling effect, humidification by itself increases the mass flow rate as well as equipment performances. So, it can be recommended to use evaporative coolers even for the weather which may not require evaporative cooler from its cooling effect viewpoint.

## References

- Bassily A. (2001). Performance improvements of the intercooled reheat regenerative gas turbine cycles using indirect evaporative cooling of the inlet air and evaporative cooling of the compressor discharge. *Proceedings of the Institution of Mechanical Engineers, Part A: Journal of Power and Energy*, Vol. 215, pp. 545-557. <https://doi.org/10.1243/0957650011538794>
- Borgnakke C., Sonntag R. E. (2016). Fundamentals of thermodynamics. *Wiley Global Education*.
- Carmona J. (2015). Gas turbine evaporative cooling evaluation for Lagos–Nigeria. *Applied Thermal Engineering*, Vol. 89, pp. 262-269. <https://doi.org/10.1016/j.applthermaleng.2015.06.018>
- Cataldi G., Güntner H., Matz C., McKay T., Hoffmann J., Nemet A., Lecheler S., Braun J. (2006). Influence of high fogging systems on gas turbine engine operation and performance. *Journal of Engineering for Gas Turbines and Power*, Vol. 128, pp. 135-143. <https://doi.org/10.1115/1.1926313>
- Chaker M., Meher-Homji C. B., Mee T. (2002). Inlet fogging of gas turbine engines: Part A—fog droplet thermodynamics, heat transfer and practical considerations. *ASME Turbo Expo 2002: Power for Land, Sea, and Air. American Society of Mechanical Engineers*, pp. 413-428. <https://doi.org/10.1115/GT2002-30562>
- De Lucia M., Lanfranchi C., Boggio V. (1995). Benefits of compressor inlet air cooling for gas turbine cogeneration plants. *ASME 1995 International Gas Turbine and Aeroengine Congress and Exposition. American Society of Mechanical Engineers*, pp. V004T011A005-V004T011A005. <https://doi.org/10.1115/95-GT-311>
- Gulotta T. M., Guarino F., Cellura M., Lorenzini G. (2017). Constructural law optimization of a boiler. *International Journal of Heat and Technology*, Vol. 35, No. 1, pp. 261-S269. <https://doi.org/10.18280/ijht.35Sp0136>
- Gulotta T. M., Guarino F., Mistretta M., Cellura M., Lorenzini G. (2018). Introducing exergy analysis in life cycle assessment: A case study. *Mathematical Modelling of Engineering Problems*, Vol. 5, No. 3, pp. 139-145. <https://doi.org/10.18280/mmep.050302>
- Ibrahim T. K., Basrawi F., Awad O. I., Abdullah A. N., Najafi G., Mamat R., Hagos F. Y. (2017). Thermal performance of gas turbine power plant based on exergy analysis. *Applied Thermal Engineering*, Vol. 115, pp. 977-985. <https://doi.org/10.1016/j.applthermaleng.2017.01.032>
- Mohapatra A. (2013). Analytical investigation of parameters affecting the performance of cooled gas turbine cycle with evaporative cooling of inlet air. *Arabian Journal for Science & Engineering (Springer Science & Business Media BV)*, Vol. 38. <https://doi.org/10.1007/s13369-013-0598-x>
- Najjar Y. S. (1996). Enhancement of performance of gas turbine engines by inlet air cooling and cogeneration system. *Applied Thermal Engineering*, Vol. 16, pp. 163-173. [https://doi.org/10.1016/1359-4311\(95\)00047-H](https://doi.org/10.1016/1359-4311(95)00047-H)
- Poullikkas A. (2005). An overview of current and future sustainable gas turbine technologies. *Renewable and Sustainable Energy Reviews*, Vol. 9, pp. 409-443. <https://doi.org/10.1016/j.rser.2004.05.009>

- Wang F., Chiou J. S. (2004). Integration of steam injection and inlet air cooling for a gas turbine generation system. *Energy Conversion and Management*, Vol. 45, pp. 15-26. [https://doi.org/10.1016/S0196-8904\(03\)00125-0](https://doi.org/10.1016/S0196-8904(03)00125-0)

